Design and Characterization of Novel Paper-based Inkjet-Printed RFID and Microwave Structures for Telecommunication and Sensing Applications

Li Yang and Manos M. Tentzeris

Georgia Electronic Design Center, School of Electrical and Computer Engineering,
Georgia Institute of Technology, Atlanta, GA 30332-0250, USA

E-mail: liyang@ece.gatech.edu

***Abstract* — In this paper, inkjet-printed microwave circuits fabricated on paper-based substrates were investigated, as a system-level solution for ultra-low-cost mass production. The RF characteristics of the paper-based substrate were studied by using the cavity resonator method and the Transmission Line method in order to characterize the dielectric constant (ε_r) and loss tangent (tanδ) of the substrate. A UHF RFID tag module was then developed with the inkjet-printing technology which could function as a technology for much simpler and faster fabrication on/in paper. Simulation and well-agreed measurement results verify a good performance of the tag module. In addition, for the first time, the possibility of paper-based substrate for multilayer microwave structures was explored, and a 2.4GHz multilayer patch resonator bandpass filter with insertion loss < 0.6dB was demonstrated. These results show that the paper material can serve for the purpose of economical multilayer structures for telecommunication and sensing applications.**

***Index Terms* — RFID, sensor, organic-substrate, dielectric characterization, multilayer, inkjet-printing, paper.**

I. Introduction

As the demand for low cost, flexible and efficient electronics increases, the materials and integration techniques become more and more critical and face more challenges, especially with the ever growing interest for “cognitive intelligence” and wireless applications, such as Radio Frequency Identification (RFID) and Wireless Local Area Networks (WLAN), such as WiFi and WiMax. For an optimal RF performance, substrate material characterization for electronics such as antennas, filters and transmission lines becomes a must, especially for low-cost materials.

In this paper, for the first time, paper-based electronics are investigated for UHF frequency band. Paper is considered one of the best organic-substrate candidates for UHF and microwave applications such as RFID/sensing. It is not only environmentally friendly, but can also undergo large reel-to-reel processing. In terms of mass production and increased demand, this makes paper the lowest cost material made. Paper also has low surface profile with appropriate coating. This is very crucial since fast printing processes, such as direct write methodologies, can be utilized instead of metal etching techniques. A fast process, like inkjet printing, can be used efficiently to print electronics on/in paper substrates.

In this effort, a cavity resonator method was utilized for the dielectric constant characterization, and a Transmission Line (TL) method was utilized for the loss tangent (tanδ) extraction. An RFID tag module using inductively coupling mechanism for the matching of the antenna to the Integrated Circuit (IC) was designed and printed on a paper substrate using conductive paste inkjet-printing, and characterized experimentally. In addition, a two-layer 2.4 GHz patch resonator bandpass filter (BPF) for WLAN applications was designed and printed on a multilayer paper configuration.

II. RF Characteristics of Paper-based Substrate

A. Dielectric Constant

The most precise methods for determining the substrate dielectric constant are resonator methods, such as microstrip ring resonators, parallel plate resonators and cavity resonators [1]. The cavity resonator method doesn’t require a pretreatment on the substrate, and provides a higher level accuracy compared with the other methods.

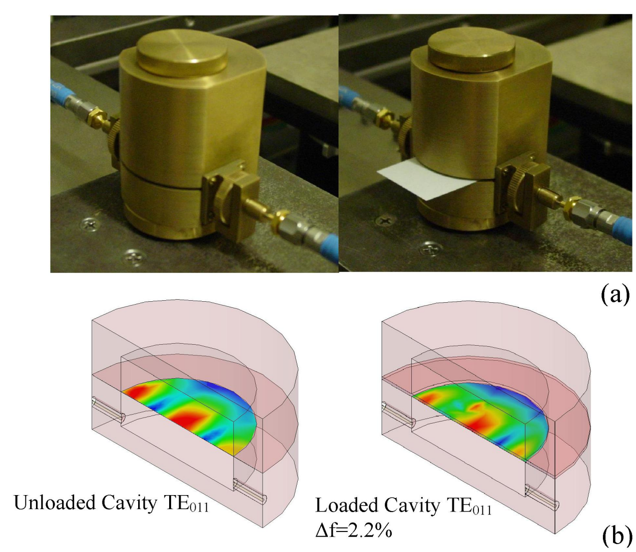

Fig. 1. (a) Photograph of the split-cylinder cavity in unloaded and loaded status. (b) The simulated field distributions to help identifying the correct resonant peak corresponding to TE_{011} mode.

1-4244-0688-9/07/$20.00 ©2007 IEEE

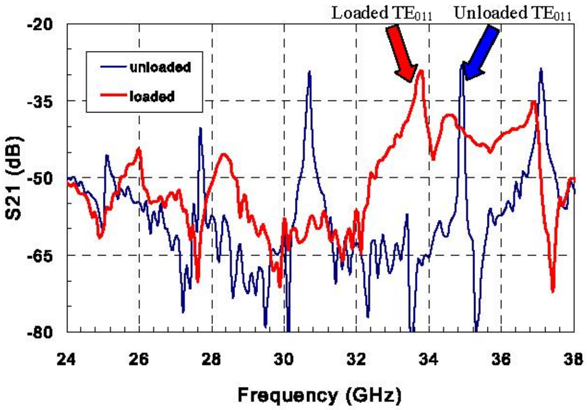

Fig. 2. Measured modes shifting of the unloaded/loaded split-cylinder cavity.

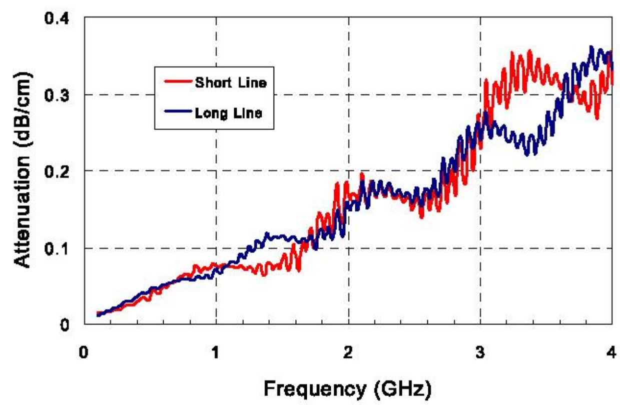

Fig. 3. Measured dielectric loss of a hydrophobic paper using Transmission Line method.

A split-cylinder resonator was fabricated with a circular-cylindrical cavity of radius 6.58mm and length 7.06mm, separated into two halves by a variable gap height which is adjustable to the thickness of the paper substrate being characterized. The feeding structure is composed of coaxial cables terminated in coupling loops. A TE_{011} resonant mode was excited in the cavity at

$$f_{011} = \frac{3\times10^8}{2\pi}\sqrt{(\frac{3.8317}{a})^2 + (\frac{\pi}{L})^2} \qquad (1)$$

where a is the cavity radius and L is its length.

A hydrophobic paper was selected for the convenience of inject-printing and to enhance durability, and placed in the gap between the two cylindrical-cavity sections. The thickness of the paper was 263um. The existence of the inserted substrate caused the shifting of the TE_{011} resonant mode. Using the resonance and boundary conditions for the electric and magnetic fields, the substrate's dielectric constant can be calculated from the shifting [2]. The full wave electromagnetic solver HFSS was used to assist identifying the correct position of the TE_{011} resonant peak, as shown in Fig. 1.

The measurement data of the resonant modes shifting is plotted in Fig. 2. For the empty cavity, the dominant mode TE_{011} was observed at 34.54GHz. After the paper sample was inserted, the TE_{011} shifted down to 33.78GHz. In this way, the sample dielectric constant of $\varepsilon_r = 1.6$ was determined. In the case where paper needs to be compressed, such as in multilayer configurations or in a laminating process, the dielectric constant will increase with increasing density. To verify this, the same paper sample was laminated to 175um thickness, and $\varepsilon_r = 2.2$ was observed. Since the previous characterization of other organic substrates performed by National Institute of Standards and Technology (NIST) features a very flat response of relative permittivity over wide frequency ranges [3], these results are also expected to be effective for very wide frequency bands.

B. Loss Tangent

In order to extract the total losses of the dielectric property of paper, a TL method was utilized. In this method the dielectric loss of a microstrip line a_d can be extracted, which provides the tanδ according to the formula [1]

$$\tan\delta = \frac{a_d \lambda_0 \sqrt{\varepsilon_e}(\varepsilon_r - 1)}{\pi\varepsilon_r(\varepsilon_e - 1)} \qquad (2)$$

where λ_0 is the free space wavelength, ε_e is the effective dielectric constant, and ε_r is the relative dielectric constant. Simulation results for conductor and radiation losses, a_c and a_r respectively, of the microstrip lines were subtracted from the total loss a_{tot}. This was done by simulating a microstrip line with no dielectric loss in HFSS and extracting a_r and a_c, then subtracting these effects from the total measured loss.

Two microstrip lines of lengths 111.8mm and 74.8mm, with width 2.53mm were measured on the same paper material of 1.2mm thickness. Since the conductivity of the conductive ink is a variable of the curing temperature, 18um thick copper was selected as the metallic material on the paper substrate at this measurement only, in order to accurately model and de-embed the conductive loss of the microstrip lines.

Measurements were recorded over a frequency range from 0.1GHz to 4GHz using Agilent 8530A Vector Network Analyzer (VNA). The feeding to the microstrip lines were performed with typical SMA connectors. The calibration method used was SOLT. Fig. 3 shows the plot of attenuation against frequency. The two measurement results agree well. The attenuation increases as expected with frequency. The attenuation was 0.061dB/cm and 0.170dB/cm at frequencies 0.9GHz and 2.4GHz respectively. These values result in a $\tan\delta = 7.7\times10^{-2}$ at 0.9GHz and $\tan\delta = 8.2\times10^{-2}$ at 2.4 GHz according to equation (2).

III. Inkjet-printed Microwave Circuits

As a first step to an all-printed paper-based electronic circuit operating at the UHF frequency band, two modules were designed and fabricated using conductive paste inkjet-printing technology. The two designs: RFID tag module and WLAN BPF are demonstrated below.

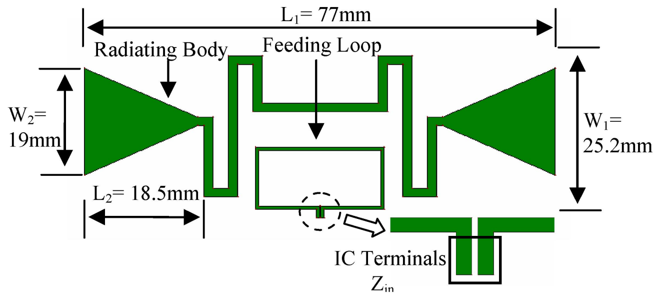

Fig. 4. Inductively coupled feeding RFID tag module configuration.

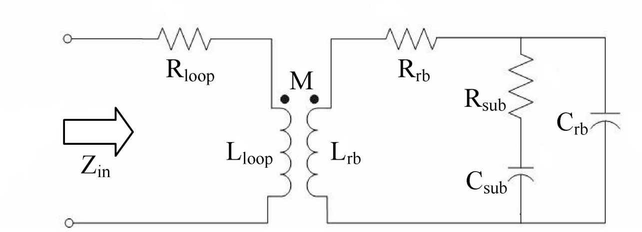

Fig. 5. Lumped element model for the inductively coupled feeding RFID tag module.

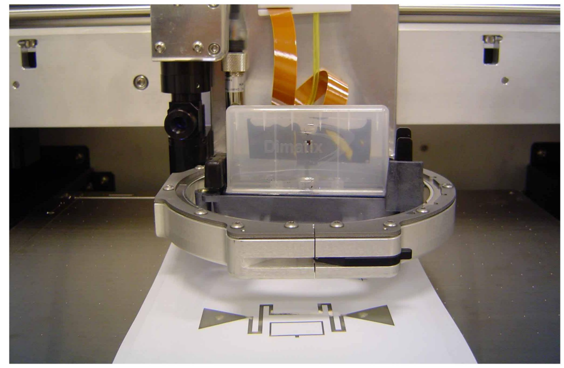

Fig. 6. Photograph of the designed RFID tag with Dimatix Materials Printer during inkjet-printing process.

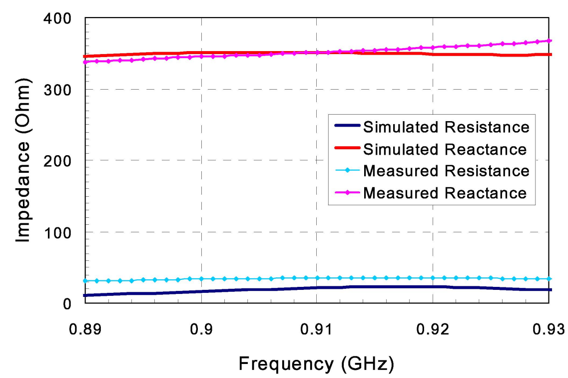

Fig. 7. Measured and simulated input resistance and reactance of the inkjet-printed RFID tag.

A. RFID Tag Module

The demand for flexible RFID tags has rapidly increased due to the requirements of automatic identification in item-level tracking. The major challenges existing in today's RFID technology advancing toward the practical level is to lower the cost of the RFID tags and reduce the design and fabrication cycle. The characterization of paper-based substrate provides the possibility to dramatically reduce the cost not only of RFID's, but also of "cognitive intelligence" sensors.

Most available commercial RFID tags are passive, and the antenna translates electromagnetic waves from the reader into power supplied to the IC. Thus, a conjugate impedance matching between the antenna and the tag IC is highly essential to power up the IC and maximize the effective range. However, most RFID ICs primarily exhibit complex input impedance with large imaginary part and very small real part, making miniaturized matching extremely challenging.

An inductively coupled feeding structure, as the proposed one shown in Fig. 4, is an effective way for impedance matching. It consists of a feed loop with two terminals and a radiating body. The two terminals of the loop are connected to the IC, and the feed "communicates" with the radiating body through mutual coupling.

The inductively coupled feeding structure can be modeled as a transformer. Fig. 5 depicts the equivalent lumped element model, where R_{rb} and R_{loop} are the individual resistances of the radiating body and the feed loop. M is the mutual inductance and L_{loop} is the self-inductance of the feed loop. R_{sub} and C_{sub} are representing the substrate effects. Without loss of generality and assuming that the substrate effect is minimal, the components of antenna input resistance R_{zin} and reactance X_{zin} at the resonant frequency can be predicted from the lumped element modeling,

$$R_{zin} = \frac{(2\pi f_0 M)^2}{R_{rb}} + R_{loop} \tag{3}$$

$$X_{zin} = 2\pi f_0 L_{loop} \tag{4}$$

Thus, at the resonant frequency, the resistance is mainly controlled by M and R_{rb}, and the reactance is dependent only upon L_{loop}. In this way, the antenna input resistance and input reactance can be adjusted independently. Therefore, inductively coupled feeding structures present one of the theoretically optimum solutions to effectively match an antenna to arbitrary IC impedances without the need of large matching circuits.

An inductively coupled feeding antenna was inkjet-printed with Dimatix Materials Printer DMP-2800, as shown in Fig. 6. The target RFID IC was Philips EPC 1.19 Gen2 RFID ASIC IC which has a stable impedance performance of 16-j350 Ω over 902~928MHz, covering the North America UHF RFID Band. The substrate was the previously characterized paper. To ensure the ink droplets sufficiently overlap, a 25um drop spacing was selected. After inkjet-printing, a low-temperature sintering step guaranteed a continuous metal conductor, providing a good percolation channel for the conduction electrons to flow. The measured and simulated RFID tag input impedance are shown in Fig. 7. Since the conductivity of the conductive ink varies from $0.4{\sim}2.5\text{x}10^7$

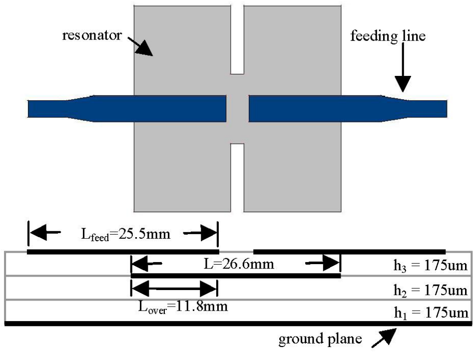

Fig. 8. Top view and side view of the proposed single-stage inkjet-printed multilayer patch resonator BPF in three layers of paper-based substrate.

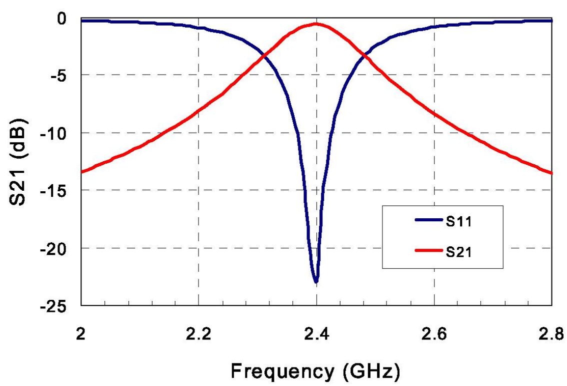

Fig. 9. Simulated S-parameters of the multilayer patch resonator BPF, with center frequency at 2.4GHz and 7% bandwidth.

Siemens/m depending on the curing temperature [4], the input resistance was slightly higher due to the additional metal loss introduced. Overall, a very good agreement was observed over the frequency band of interest.

B. Multilayer Microwave Circuit

The evolution toward portable light-weight telecommunication systems along with the increasing demand for high-density packaging technologies have led to an increasing research in multilayer technologies such as LTCC and LCP architectures. However, these applications are limited due to the relatively expensive fabrication techniques. In this aspect, paper would be an ideal candidate as an ultra-low-cost multilayer material.

In this section, a single-stage slotted-patch band pass filter for 2.4GHz WLAN application was designed and printed on/in paper-based substrate to demonstrate this novel solution. The configuration of the proposed structure is shown in Fig. 8. The square resonator was developed from the basic half-wavelength square patch at 3.8GHz by adding a 1.75mm x 8.8mm transverse cut on two sides. Transverse cuts contribute to significant additional inductance so that the operating frequency range was shifted by about 36%. Therefore, the patch size was reduced significantly. The simulation result is plotted in Fig. 9. It is revealed that the insertion loss is < 0.6dB. The

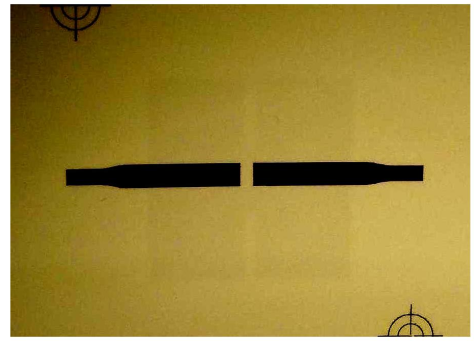

Fig. 10. Photograph of the single-stage inkjet-printed multilayer patch resonator BPF after the laminating process. The cross hair pattern is used for alignment.

bandwidth extends from 2.31GHz to 2.48GHz, which is about 7%.

The circuit layout on each layer was inkjet-printed independently at the first step. After alignment, the PHI laminator Q-247C4 was utilized for the bonding process, while 10 tons RAM force was applied under 200 ºF. The fabricated multilayer patch resonator BPF is shown in Fig. 10. This is the first time an ultra-low-cost multilayer circuit on paper-based substrate has been demonstrated. It has to be noted that a paper-based multilayer technology would allow for the light-weight miniaturization of "cognitive" sensing devices, through the embedding of IC's, as well as of printed batteries, sensors and power scavenging devices.

IV. CONCLUSION

The RF characteristics of paper-based substrates have been investigated for the first time in UHF frequency band, and two benchmarking inkjet-printed topologies have been fabricated and tested. Our effort demonstrates that inkjet printing, as a fast process, can be used efficiently to print UHF and RF electronics on or in paper substrates. A compact RFID tag module, using inductively coupling mechanism for the matching of the antenna to the IC, was designed and printed on a paper-based substrate featuring a very good performance. Paper-based multilayer structures were also explored. These technologies could pave the way for simple, low-cost, system-level packaging structures for telecommunication and sensing applications.

REFERENCES

[1] D. Thompson, G. Ponchak, M. M. Tentzeris, J. Papapolymerou, "Characterization of LCP material and transmission lines on LCP substrates from 30 to 110GHz," *IEEE Trans. Microwave Theory & Tech.*, vol. 52, no. 4, pp. 1343-1352, April 2004.

[2] G. Kent, "An evanescent-mode tester for ceramic dielectric substrates," *IEEE Trans. Microwave Theory & Tech.*, vol. 36, no. 10, pp. 1451-1454, October 1998.

[3] M. Janezic, "Nondestructive relative permittivity and loss tangent measurements using a split-cylinder resonator," *2003 Doctor of Philosophy Thesis, Univ. Colorado*, 2003.

[4] Cabot Corporation, "Inkjet silver conductor AG-IJ-G-100-S1," *Data Sheet*, October 2006.